Combustion of a Single Droplet in the Presence of an Oscillating Flow

Man Yeong Ha* and Sun Kie Kim*

(Received August 8, 1994)

The two-dimensional, unsteady, laminar conservation equations for mass, momentum, energy and species transport in the gas phase are solved numerically in spherical coordinates. This is to study the heat and the mass transfer, and the combustion around a single spherical droplet. The droplet mass and momentum equations are also solved simultaneously with the gas phase equations in order to investigate the effects of droplet entrainment in the oscillating flow with and without a steady velocity. The numerical solution for a single droplet combustion gives the droplet diameter variation as well as the gas phase velocity, temperature and species concentrations as a function of time. The effects of frequency, amplitude of oscillating flow, velocity ratio of oscillating flow amplitude to the steady velocity, ambient temperature and initial droplet diameter on the droplet combustion are also investigated. The droplet burning history is not governed by the d^2-law in the presence of oscillating flow, unlike to the case under quiescent ambient conditions.

Key Words: Droplet Combustion, Oscillating Flow, Numerical Computation, d^2-Law

Nomenclature

c_p : Specific heat
d : Droplet diameter
D_v : Binary diffusion coefficient
E : Activation energy
f : Frequency
i : Static enthalpy
k : Thermal conductivity
K : Frequency factor
L : Heat of gasification for unit mass of fuel
m_l : Droplet mass
$\dot{m}_l''$: Net mass flux
P : Pressure
Q : Heat of combustion for unit mass of fuel
r : Radial position
R^0 : Universal gas constant
Re : Reynolds number $|U-v_l|D/\nu$
S_ϕ : Source term for general variable ϕ
t : Time
T : Temperature
u_r : Radial velocity
u_θ : Axial velocity
U_0 : Steady slip velocity
U_1 : Acoustic peak velocity
v_l : Droplet velocity
W : Reaction rate
W_0 : Molecular weight of oxidizer
Y_i : Mass fraction of species i
Γ_ϕ : Diffusivity for general variable ϕ
σ : Stoichiometric fuel-oxidizer mass ratio
θ : Angular direction
μ : Viscosity
ρ : Gas density
ϕ : General variable given in equation (1)
∞ : Infinity

Subscripts

bn : Boiling
F : Fuel
l : Droplet
P : Product
g : Gas

* Research Institute of Mechanical Technology School of Mechanical Engineering Pusan National University
30 Changjeon-Dong, Kumjeong-Ku, Pusan 609-735, Korea

O : Oxidizer
r : Radial
w : Wall
0 : Initial
θ : Angular
ϕ : Dependent variables
∞ : Infinity

1. Introduction

The effect of an oscillating flow field with and without a steady component on heat and mass transfer from a single spherical particle and droplet has been a topic of investigation since the late 1930s(Marthelli & Boelter, 1939). Some examples of these theoretical and experimental studies can be found in refs.(Baxi & Ramachandran, 1969, Mori et al., 1969, Gibert & Angelino, 1974, Larsen & Jensen, 1978, Rawson, 1988). These publications report an increase, decrease or unnoticeable change in heat and mass transfer, depending on the frequency and the magnitude of the steady and oscillating flow.

Zinn et al.(1982) and Faeser(1984) indicate the positive effects of high intensity acoustics on coal combustion by using acoustic drivers or pulsed combustion. Koopmann et al.(1989) investigated the effects of high intensity acoustic fields on the rate of combustion of coal-water slurry fuel in the sonic combustor. Yavuzkurt & Ha(1991) and Yavuzkurt et al.(1991) calculated a decrease of 15.7% and 12.1%, respectively, in the char burnout length for a sound pressure level of 160 dB and at a frequency of 2000 Hz compared to the case with no sound for the combustion of 100 μm pulverized coal or coal-water slurry fuels. Ha and Yavuzkurt(1991) investigated in details the effects of high intensity acoustic fields on heat and mass transfer, combustion around a single spherical carbon or char particle. They solved the gas phase equations simultaneously with the particle phase equations in order to consider the effects of particle entrainment on the particle combustion.

For droplet combustion, Law(1982) gave a detailed explanation of the fundamental mechanisms governing the vaporization and combustion of an isolated, single spherical droplet in a spray of liquid or slurry fuel. This review paper described the usefulness and limitations of d^2-law governing the vaporization and combustion of a single droplet under various assumptions, based on the research works(Fernandez-Pello & Law, 1982, Wu et al., 1983, Chung & Law, 1983, Chao et al., 1985) which Law's group carried out. The effects of variable properties and kinetics on the flame structure were also discussed. Faeth(1983) developed locally homogeneous flow(LHF) and separated flow(SF) models to explain the detailed structure of the flow for the two- or three-dimensional spray systems found in furnaces, gas turbine combustors, internal combustion engines, etc.

In the previous studies on the vaporization and combustion of droplets, it is usually assumed that the droplet is stationary relative to its gaseous environment. Thus, the droplet momentum equation is not included with the constant slip velocity between the droplet and the bulk gas stream. However, in the initial stages of combustion of pulverized coal or coal-water slurry droplets, there exists a steady slip velocity, U_0. This steady slip velocity decreases during combustion since coal particles or particle agglomerates become entrained in the main gas flow. During the later stages of pulverized coal or coal-water slurry fuel combustion, the slip velocity between the entrained particles and the gas is quite low for a significant period of time, leading to low heat and mass transfer to and from the particles, as shown by Ha and Yavuzkurt(1991). For this situation, the particle or droplet momentum equation should be solved simultaneously with gas phase equations and the slip velocity continuously changes depending on the droplet trajectories.

In order to investigate heat and mass transfer, combustion past droplets entrained in an oscillating flow with a steady velocity component, an oscillating flow, $U_1\cos(2\pi ft)$, induced by the high intensity acoustic fields is superposed on the mean steady flow, U_0, in the present study. The two-dimensional, unsteady conservation of mass, momentum, energy and species equations for a laminar flow past droplets in spherical coordinates was solved simultaneously with the droplet

momentum equation. The results obtained considering droplet entrainment are compared with those without entrainment. The main purpose of this study is to investigate not only the dynamic history of burning droplets in the presence of oscillating flow fields but also to consider the direct interaction between the combustion gas and the applied acoustic field.

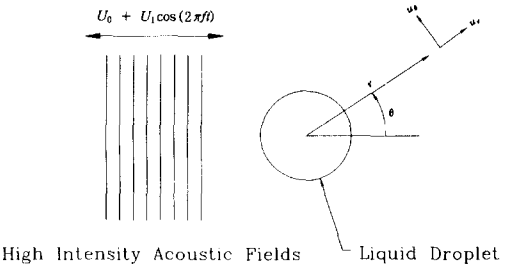

Fig. 1 Schematic diagram showing the geometry and some of the nomenclature used to simulate combustion, heat and mass transfer from a spherical droplet in the presence of oscillating flow with a steady velocity

2. Mathematical Model

2.1 Governing equations

The combustion of a single liquid droplet in the presence of high intensity acoustic fields is investigated by solving the unsteady and two-dimensional axisymmetric conservation equations for laminar flow with the following common form(see Patankar, 1980):

$$\frac{\partial}{\partial t}(\rho\phi)+\frac{1}{r^2}\frac{\partial}{\partial r}(r^2\rho u_r\phi)+\frac{1}{r\sin\theta}\frac{\partial}{\partial\theta}(\sin\theta\rho u_\theta\phi)=\frac{1}{r^2}\frac{\partial}{\partial r}\left(\Gamma_\phi r^2\frac{\partial\phi}{\partial r}\right)+\frac{1}{r^2\sin\theta}\frac{\partial}{\partial\theta}\left(\Gamma_\phi\sin\theta\frac{\partial\phi}{\partial\theta}\right)+S_\phi \quad (1)$$

The flow field and the droplet geometry with some nomenclature are shown in Fig. 1. In the conservation of momentum equation, $\phi=u_r$, u_θ represents the velocities in the radial r and angular θ directions, respectively. In the energy equation $\phi=i$ is the static enthalpy. The source terms ϕ in Eq. (1) are given in Table 1. W in Table 1 represents the rate of production of species Y_i^*. For homogeneous combustion in the gas phase, the one-step chemical reaction is modeled by the following chemical process:

$$\nu_F[F]+\nu_O[O]=\nu_P[P]+Q \quad (2)$$

Further assuming an one-step second-order irreversible Arrhenius reaction between the fuel and oxidizer, then the reaction term W in Table 1 can be expressed as(Wu et al., 1982):

$$W=-\frac{K\rho^2 Y_O Y_F\exp(-E/R^0T)}{W_0} \quad (3)$$

where Y_F and Y_O represent the mass fraction of fuel and oxidizer, respectively. In the species

Table 1 Source terms S_ϕ in equation

ϕ	Γ_ϕ	S_ϕ
u_r	μ	$-\frac{\partial p}{\partial r}+\frac{1}{r^2}\frac{\partial}{\partial r}\left(\mu r^2\frac{\partial u_r}{\partial r}\right)+\frac{1}{r\sin\theta}\frac{\partial}{\partial\theta}\left(\mu\sin\theta\frac{\partial u_\theta}{\partial r}\right)-\frac{1}{r^2\sin\theta}\frac{\partial}{\partial\theta}(\mu\sin\theta u_\theta)-\frac{2\mu}{r^2}\frac{\partial u_\theta}{\partial\theta}-4\mu\frac{u_r}{r^2}-2\mu\frac{u_\theta\cot\theta}{r^2}+\rho\frac{u_\theta}{r^2}$
u_θ	μ	$-\frac{1}{r}\frac{\partial p}{\partial\theta}+\frac{1}{r^2}\frac{\partial}{\partial r}\left(\mu r^2\frac{\partial u_\theta}{\partial r}\right)+\frac{1}{r^2\sin\theta}\frac{\partial}{\partial\theta}\left(\mu\sin\theta\frac{\partial u_\theta}{\partial\theta}\right)+\frac{2}{r\sin\theta}\frac{\partial}{\partial\theta}\left(\mu\sin\theta\frac{u_r}{r}\right)+\frac{\mu}{r}\frac{\partial u_\theta}{\partial r}+\frac{\mu}{r^2}\frac{\partial u_r}{\partial\theta}-\mu\frac{u_\theta}{r^2}-2\mu\frac{u_r\cot\theta}{r^2}-2\mu\frac{u_\theta\cot^2\theta}{r^2}-\frac{1}{r^2}\frac{\partial}{\partial r}(\mu r u_\theta)-\rho\frac{u_r u_\theta}{r^2}$
i	k/c_p	$-QW$
Y_i^*	ρD_v	$-W$

conservation equation, $\phi = Y_i^*$ is defined as :

$$Y_F^* = Y_F \quad Y_O^* = \sigma Y_O \tag{4}$$

where σ represents the stoichiometric fuel-oxidizer mass ratio. The following equation of state is used

$$\rho T = \rho_\infty T_\infty \tag{5}$$

under the assumption that the variation of the pressure is small across the boundary layer(Fernandez-Pello & Law, 1982). The quantities are allowed to vary in the radial(r) and angular(θ) directions whereas a circumferential symmetry is assumed around an axis which passes through the center of the droplet and is parallel to the flow direction. Thus, the mass, momentum, energy and species equations in the gas phase can not be decoupled due to the source terms given by Table 1 and should be solved simultaneously.

The mass conservation equation for a reacting droplet is expressed as :

$$\frac{dm_l}{dt} = -4\pi r_l^2 \dot{m}''_l \tag{6}$$

where m_l is the mass of liquid droplet and $\dot{m}''_l$ is a net mass flux from the burning droplet. The droplet momentum equation is expressed as :

$$m_l \frac{dv_l}{dt} = \Gamma_d (U - v_l) \tag{7}$$

where

$$\Gamma_d = 4\pi r_l^2 \rho C_d \mid U - v_l \mid /2 \tag{8}$$

$$C_d = \frac{24}{Re} \frac{(1 + 0.15 Re^{0.687})}{1 + B} \tag{9}$$

$$B = \frac{1}{L}\left[C_P (T_\infty - T_l) + \frac{Q Y_{O,\infty}}{\sigma} \right] \tag{10}$$

where v_l in Eq. (7) represents the droplet velocity and U represents $U_0 + U_1 \cos(2\pi ft)$ for the oscillating flow due to the acoustic field with a steady velocity. C_d in Eq. (9) represents the drag coefficient with the value given by Smith et al.(1985) with a correction due to mass loss.

2.2 Initial and boundary conditions

The conservation equations of mass, momentum, energy and species for the gas phase are given by Eq. (1) with the proper source terms to calculate the combustion of a liquid droplet in the presence of oscillating flow with a steady velocity.

At the droplet surface $r = R_l$ where R_l is the radius of the burning droplet, the velocity u_θ is zero, whereas the radial velocity u_r can be calculated as follows :

$$u_r = \frac{\dot{m}''_l}{\rho} \tag{11}$$

where $\dot{m}''_l$ is a net mass flux out of the burning droplet. The following boundary conditions are used for the energy and species conservation equations at the droplet surfaces :

$$T \mid_w = T_{bn} \tag{12}$$

$$k \frac{\partial T}{\partial r} = \dot{m}''_l L \tag{13}$$

$$\rho u_r \mid_w = \rho u_r Y_F \mid_w - \rho D_v \frac{\partial Y_F}{\partial r} \mid_w \tag{14}$$

$$\rho u_r Y_i \mid_w = \rho D_v \frac{\partial Y_i}{\partial r} \mid_w, \quad i \neq F \tag{15}$$

In the present calculations, it is assumed that the droplet has constant and uniform boiling temperature T_{bn} during combustion as shown in Eq. (12). As $r \to \infty$,

$$u_\theta = -[(U_0 + U_1 \cos(2\pi ft)] \sin\theta \tag{16}$$

$$u_r = [U_0 + U_1 \cos(2\pi ft)] \cos\theta \tag{17}$$

$$i = i_\infty \tag{18}$$

$$Y_i^* = Y_{i,\infty}^* \tag{19}$$

where U_0 is the steady velocity and U_1 is the peak value of an oscillating flow. At $\theta = 0$ and π,

$$\frac{\partial \phi}{\partial \theta} = 0 \text{(Symmetry Conditions)} \tag{20}$$

Initial conditions have the specified values.

3. Results and Discussion

The droplet mass and momentum conservation Eqs. (6) and (7) with two unknowns(r_l and v_l) are coupled to the gas phase conservation Eq. (1) with seven unknowns(u_r, u_θ, P, T, $Y_1 \sim Y_3$). Thus, strongly coupled, nonlinear, unsteady and two-dimensional conservation equations with a total of nine unknowns need to be solved simultaneously. The present calculations are made using the noninertial coordinate system in order to consider the moving droplet due to entrainment, and using a coordinate transformation which fits to a shrinking droplet, as explained by Ha(1990). The gas phase equations are first solved using the

same SIMPLEC procedure of Doormaal and Raithby(1982). Using this solution, the droplet conservation equations are solved to yield the updated source terms for the gas phase, since the droplet is reacting. The gas phase equations are solved again using these updated source terms, establishing the new solution for the gas field. This iterative procedure is repeated until the convergence criteria for the gas phase equations, and for the droplet temperature.

These solutions give the droplet diameter variation as functions of time. The unsteady two-dimensional(2-D) code with chemical reactions also calculates the oscillating velocity, temperature and species fields in the gas surrounding the burning droplet. All the calculations are made using the simulation conditions given by Aggarwal and Sirignano(1985) as shown in Table 2. The limiting case of droplet combustion in a quiescent environment($U_0=U_1=0$) is simulated using the present laminar, unsteady and two-dimensional computer code. Williams(1976) and Kanury(1977) gives d^2-law for the droplet combustion in a quiescent environment defined as:

$$d_l^2=d_0^2-K_b t \tag{21}$$

where

$$K_b=\frac{8k}{C_P\rho_l}ln(1+B) \tag{22}$$

A comparison of droplet burning history in a quiescent environment obtained from the present simulation with d^2-law given in Eq. (21) gives about 5% difference in burnout time. We think that this difference occurs due to the difference of the assumptions used in the present simulations and d^2-law:

(1) No solution for the gas phase momentum equation is needed with constant pressure in the d^2-law, whereas the momentum equation given in Eq. (1) with source terms in Table 1 is solved in the present simulation.

(2) The infinitely fast chemical kinetics are used in the d^2-law, whereas the chemical kinetics of finite rates in the present simulations.

(3) The quasi-steady solutions are obtained in the d^2-law, whereas the unsteady solution in the present simulations.

After the benchmarks made in a quiescent

Table 2 Values of various parameters used in the combustion of single droplet in the presence of high intensity acoustic fields

Parameter	Value
c_{pg}	(Gas Specific Heat) 1046.5 J/kgK
c_{pl}	(Liquid Specific Heat) 2209.2 J/kgK
L	(Heat of vaporization) 322140 J/kgK
M_a	(Air molecular weight) 28.9 kg/kmole
M_f	(Fuel molecular weight) 142.3 kg/kmole
M_O	(Oxygen molecular weight) 32 kg/kmole
P	(Initial pressure) 1 atm
Q	(Heat of combustion) 311680 J/kg
T_a	(Activation temperature) 15096.85 K
T_{bn}	(Normal boiling tempearture for the fuel) 447 K
T_∞	(Surrounding gas temperature) 1500 K
$\mu_g=\rho D_v$	(Gas viscosity) 1.844E-5 kg/ms
ρ_l	(Liquid density) 730 kg/m3
k_g	(Gas conduction coefficient) 0.01929746 W/mK

environment, the program was run for the case of an oscillating flow with and without a steady flow around a burning spherical droplet.

Figure 2 shows the oscillating flow U, the entrained droplet velocity v_l and the relative velocity($U-v_l$) at 50 Hz without a steady flow($U_0=0$). The applied acoustic field U oscillates with an amplitude of 40 m/s. During the droplet combustion, the droplet is entrained in an oscillating flow with a phase lag. Even if the droplet oscillates with an amplitude of velocity, the relative velocity($U-v_l$) of oscillation has an amplitude slightly lower than that of the oscillating flow U due to the phase lag which exists during a significantly long time, as shown in Fig. 2. With decreasing droplet diameter during combustion, the amplitude of droplet velocity increases and the phase lag decreases, resulting in decreasing relative velocity($U-v_l$). This relative velocity determines the combustion rate of a single droplet.

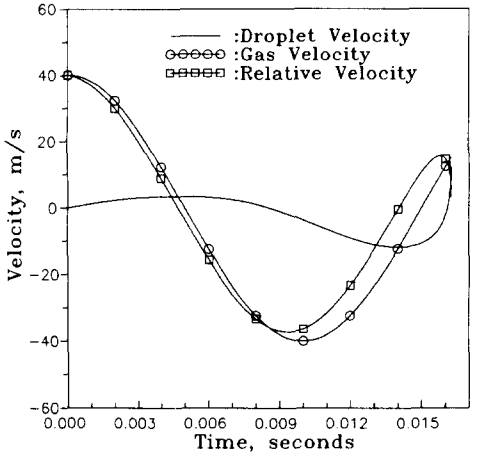

Fig. 2 Droplet velocity, surrounding steady velocity and relative velocity as a function of time : $U_0=0$, $U_1=40$ m/s, f=50 Hz, $d_0=105$ μm

Figure 3 shows the velocity vectors around burning droplet for the frequency of 50 Hz at the time of 4.99, 9.99 and 14.99 ms. The enlarged view close to the droplet surface is also shown in the circle of Fig. 3. The relative velocity($U-v_l$) at t =4.99 ms is −3.3 m/s(see Fig. 2) with a flow

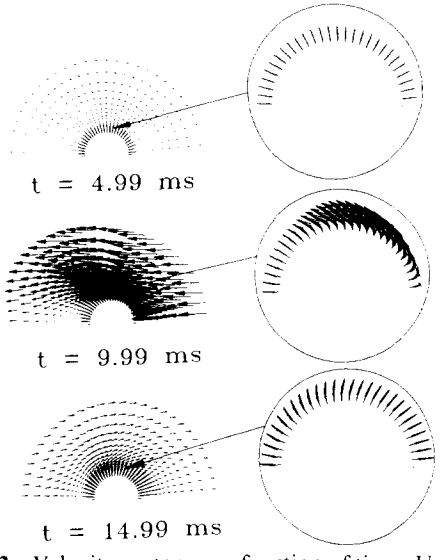

Fig. 3 Velocity vectors as a function of time : $U_0=0$, $U_1=40$ m/s, f=50 Hz, $d_0=105$ μm

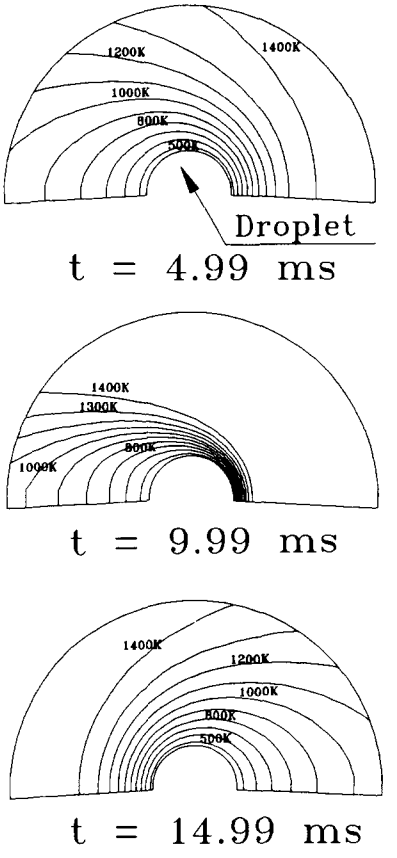

Fig. 4 Constant temperature lines as a function of time : $U_0=0$, $U_1=40$ m/s, f=50 Hz, $d_0=105$ μm

direction from right to left. The droplet diameter at this time is about 80% of initial droplet diameter($d_0=105\ \mu$m). At $t=9.9$ ms, the flow direction is from right to left with a relative velocity of -36.4 m/s and with about 55% of initial droplet diameter. The flow direction at $t=14.99$ ms changes from left to right with a relative velocity of 10.5 m/s and with about 21% of initial droplet diameter. The flow fields around the burning droplet show different shapes from those around a solid sphere, due to the blowing(mass transfer on the droplet surface) during droplet combustion.

Figure 4 shows the isothermal lines for the frequency of 50 Hz at the time of 4.99, 9.99 and 14.99 ms. These lines extend from $500K$ close to the droplet surface and continue to $1400K$, with intervals of $100K$. At $t=4.99$ and 9.99 ms, the flow direction is from right to left and high temperature gradients are observed around the leading half of the droplet from $\theta=0$ to 90, particularly near the stagnation point($\theta=0$). When the flow direction is reversed at $t=14.99$ ms, the stagnation point is located at $\theta=180$ and the location of higher temperature gradient is reversed. The absolute magnitude of relative velocity at $t=14.99$ ms is about three times larger than that at $t=4.99$ ms. However, the boundary layer thickness for temperature at $t=14.99$ ms is similar to that at $t=4.99$ ms due to increased blowing during droplet combustion. The iso-lines for fuel mass fraction Y_F and oxidizer mass fraction Y_O have similar profiles to isothermal lines.

Figures 5(a) and 5(b) show the net mass flux $\dot{m}''_t$ and squared droplet diameter as a function of time. The net mass flux from the burning droplet increases with decreasing droplet diameter, due to the increased heat transfer rate to the droplet as given in Eq. (13). The net mass flux from the burning droplet also depends on the absolute magnitude of the relative velocity, giving decreasing net mass flux with decreasing absolute magnitude of relative velocity. Thus the combined effects of the droplet diameter and the absolute magnitude of the relative velocity determine the net mass flux from the burning droplet as shown in Fig. 5(a). The results with droplet entrainment

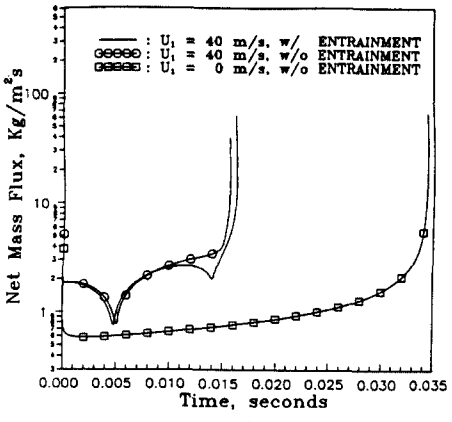

(a)

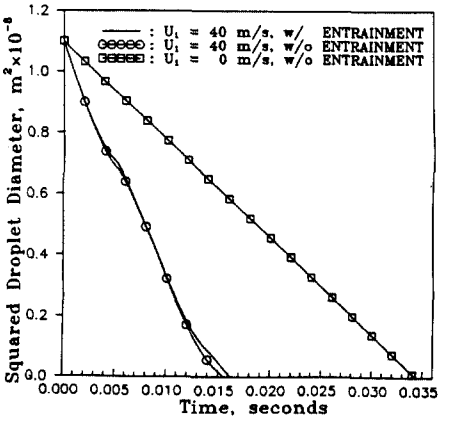

(b)

Fig. 5 (a) Net mass flux and (b) squared droplet diameter as a function of time in a quiescent environment and at $U_1=40$ m/s with and without entrainment : $U_0=0$, $d_0=105\ \mu$m

are compared to those without entrainment and also with those in the quiescent ambient conditions. The relative velocity without entrainment in an oscillating flow is the same as the oscillating flow U. Thus the absolute magnitude of relative velocity with entrainment is lower than that without entrainment, as shown in Fig. 2. The droplet burnout time in an oscillating flow is about 16.2 ms. Compared to the case under quiescent ambient conditions, the decrease in droplet combustion time is about 52.9% with droplet entrainment and 54.6% without droplet entrainment in an oscillating flow($f=50$ Hz, $U_0=0$, $U_1=40$), yielding slightly increased burn-out times

with droplet entrainment at 50 Hz. The difference in droplet combustion time with and without entrainment is about 3.7%. Under quiescent ambient conditions, the droplet burning history follows d^2-law. However, depending on the magnitude of the relative velocity in an oscillating flow, the deviation from the d^2-law for the burning history both with and without entrainment is large under the condition of $f=50$ Hz, $U_0=0$ and $U_1=40$.

Figure 6 shows the entrained droplet velocity v_l, the oscillating flow U, and the relative velocity$(U-v_l)$ at 50 and 2000 Hz, in order to investigate the frequency effect on the droplet combustion. Figures 7(a) and 7(b) show the net mass flux $\dot{m}''_l$ and squared droplet diameter as a function of time. When the frequency is increased to 2000 Hz, the droplet oscillates with a small amplitude compared to the amplitude of the oscillating flow

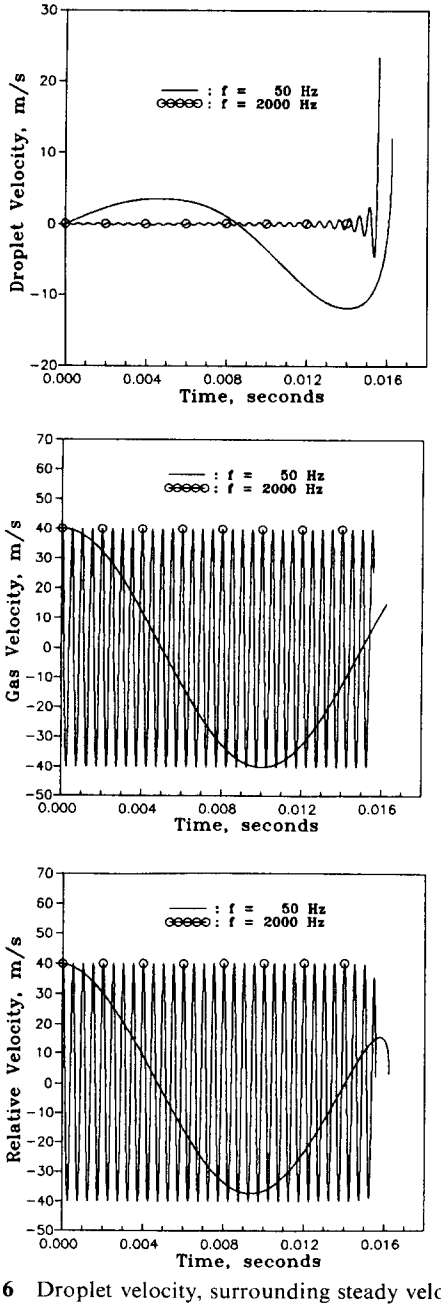

Fig. 6 Droplet velocity, surrounding steady velocity and relative velocity as a function of time for frequencies of 50 and 2000 Hz : $U_0=0$, $U_1=$ 40 m/s, $d_0=105$ μm

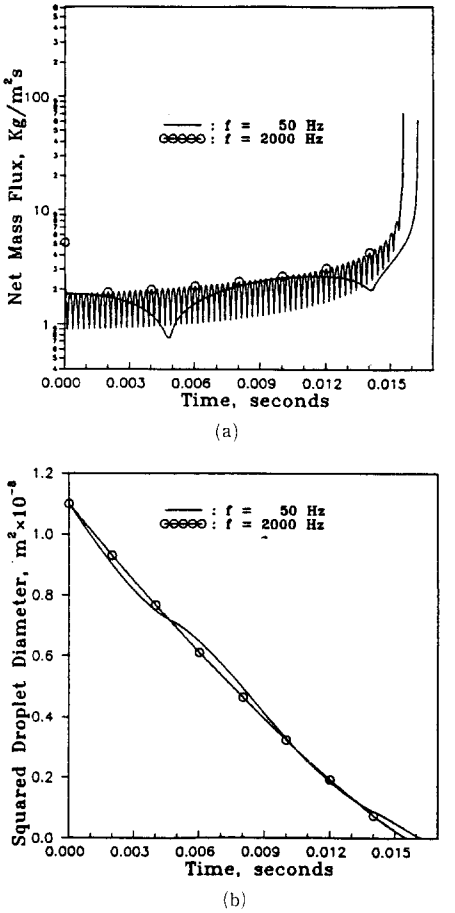

Fig. 7 (a) Net mass flux and (b) squared droplet diameter as a function of time for frequencies of 50 and 2000 Hz : $U_0=0$, $U_1=40$ m/s, $d_0=$ 105 μm

U, except towards the very end of combustion process as shown in Fig. 6. The phase lag between U and v_l increases with increasing frequency from 50 to 2000 Hz. The relative velocity($U-v_l$) of oscillation has almost the same amplitude as the oscillating flow U at 2000 Hz, giving almost the same net mass flux and droplet combustion time with and without droplet entrainment. The droplet combustion time at 50 and 2000 Hz is about 16.2 ms and 15.6 ms. These show that a high frequency is preferable to a low frequency as far as the reduction in the droplet burnout time is concerned. The droplet burning history has different profiles from d^2-law for both frequencies of 50 and 2000 Hz, as shown in Fig. 7(b).

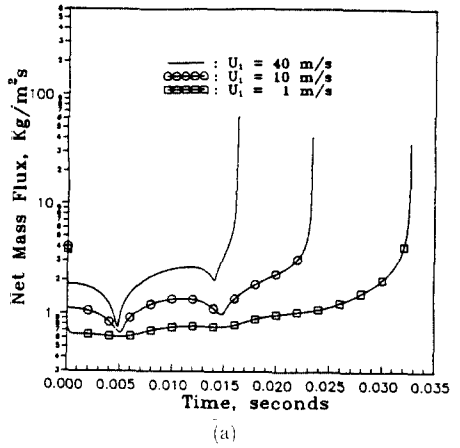

(a)

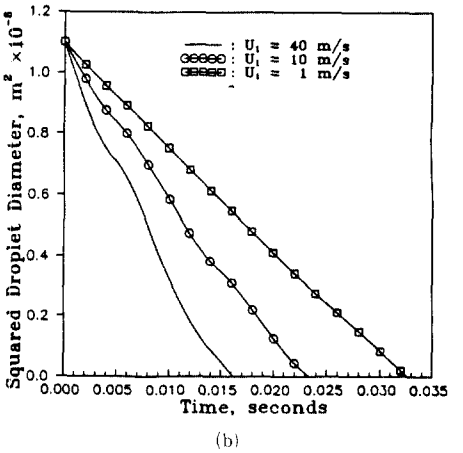

(b)

Fig. 8 (a) Net mass flux and (b) squared droplet diameter as a function of time at $U_1=1$, 10 and 40 m/s : $U_0=0$, f=50 Hz, $d_0=105$ μm

Figures 8(a) and 8(b) show the net mass flux $\dot{m}''_l$ and squared droplet diameter as a function of time, in order to consider the effects of the amplitude U_1 of the oscillating flow($f=50$ Hz, $U_0=0$) on the droplet combustion. The convective heat and mass transfer increases due to the increase in the relative velocity with increasing U_1 during combustion. Thus, the net mass flux increases and the combustion time decreases with increasing U_1. The droplet burning time with $U_1=1$, 10 and 40 is 32.6, 23.4 and 16.2 ms, respectively. When $U_1=1$, the droplet burning history follows d^2-law. However, the deviation from d^2-law increases with increasing U_1.

In order to investigate droplet combustion entrained in an oscillating flow with a steady velocity component, an oscillating flow, $U_1\cos(2\pi ft)$, induced by the high intensity acoustic fields is superposed on the mean steady velocity, U_0. The entrained droplet velocity v_l, the oscillating flow U, and the relative velocity($U-v_l$) at the frequency of 50 Hz are shown in Fig. 9. In order to consider the effects of velocity ratio(U_1/U_0) on the droplet combustion, the amplitude of oscillating flow varies with $U_1=0$, 10, 20, 40, 80 and 120 for the fixed steady value($U_0=40$). We also considered the case with $U_0=0$ and $U_1=40$. The magnitude of relative velocity determines the heat and mass transfer and combustion of liquid droplet entrained in an oscillating flow, giving the net mass flux and squared droplet diameter as a function of time as shown in Figs. 10 and 11, respectively. The burnout times for $U_0=40$ with varying amplitude of oscillating flow are 14.5 ms($U_1=0$), 14.96 ms($U_1=10$), 15.69 ms($U_1=20$), 15.65 ms($U_1=40$), 11.84 ms($U_1=80$) and 10.13 ms($U_1=120$), respectively. When $U_0=0$ and $U_1=40$, the combustion time is 16.23 ms. The flow direction of steady velocity is one direction from left to right but the direction of oscillating flow changes as a result of acoustic field. The absolute magnitude of this steady and oscillating velocity, $U_0+U_1\cos(2\pi ft)-v_l$, determines heat and mass transfer from a burning droplet. When $U_1<U_0$, the combustion time mainly depends on the magnitude of steady velocity and increases slightly with increasing U_1 for $U_0=40$, compared to the

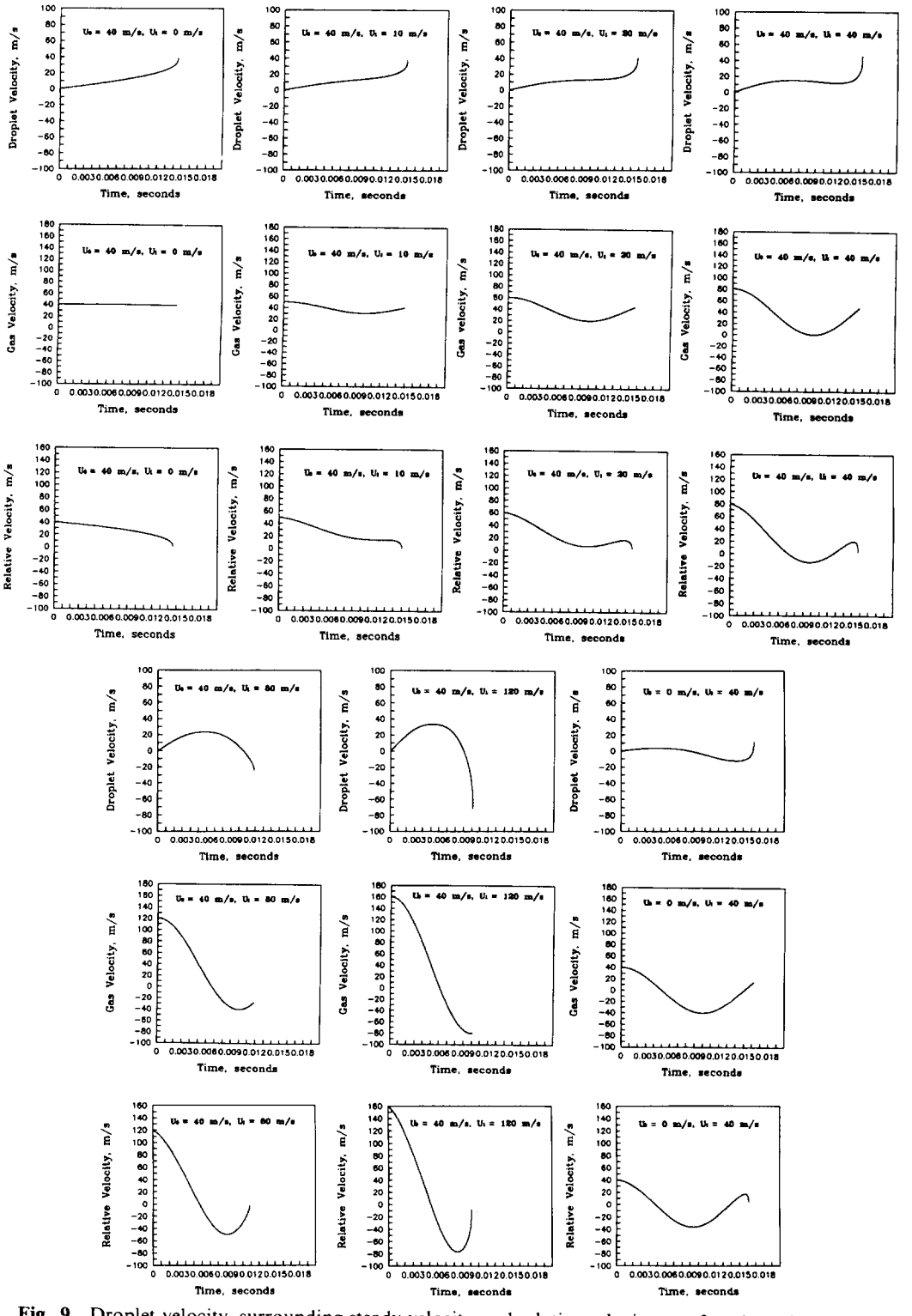

Fig. 9 Droplet velocity, surrounding steady velocity and relative velocity as a function of time for various values of U_0 and U_i : f=50 Hz, d_0= 105 μm

combustion time with $U_0=40$ and $U_1=0$. However, when $U_1 > U_0$, increasing the oscillating velocity superposed on a steady component creates a larger average slip velocity between the droplet and surrounding gas, resulting in increased heat and mass transfer and combustion as compared to the case of steady flow only($U_0=40$ and $U_1=0$). Ha and Yavuzkurt(1993) show the similar results for the heat transfer from a stationary spherical sphere in the presence of oscillating flow with a steady velocity.

Figure 12 shows the entrained droplet velocity v_l, the oscillating flow U, and the relative velocity $U-v_l$ when the frequency is increased to 2000 Hz. The magnitude of relative velocity determines the net mass flux and squared droplet diameter as

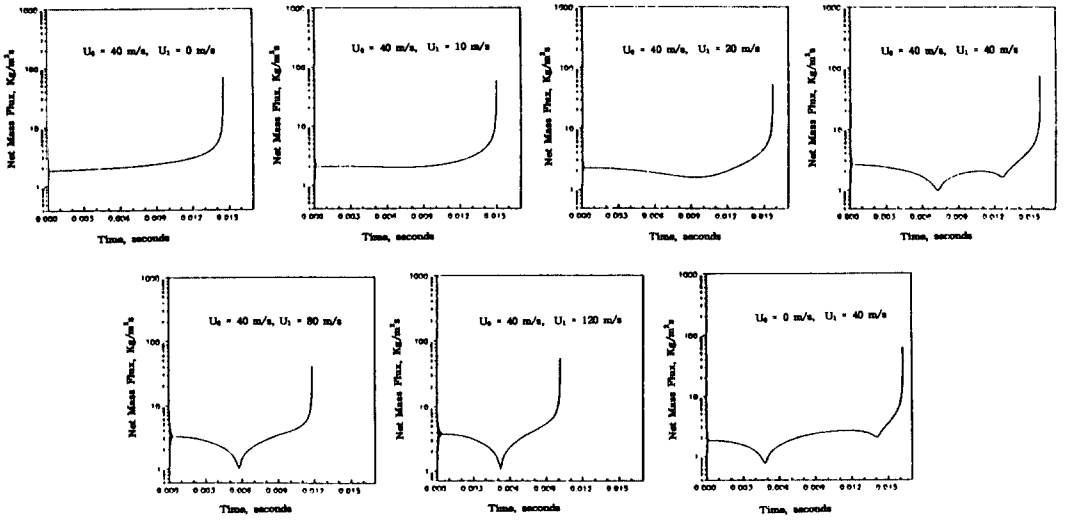

Fig. 10 Net mass flux as a function of time for various values of U_0 and U_1 : f=50 Hz, $d_0=105$ μm

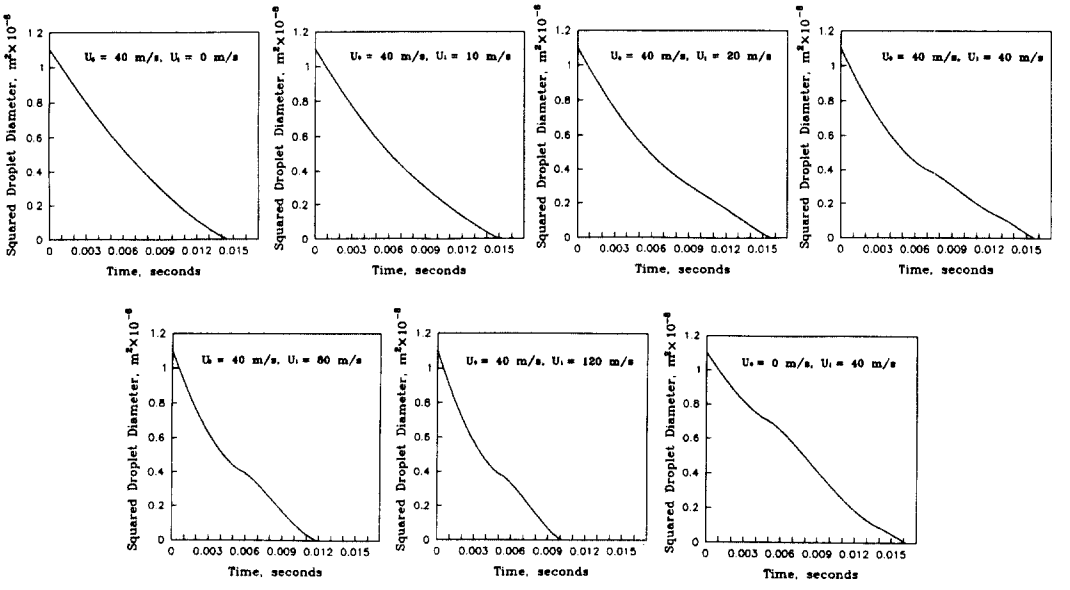

Fig. 11 Squared droplet diameter as a function of time for various values of U_0 and U_1 : f=50 Hz, $d_0=105$ μm

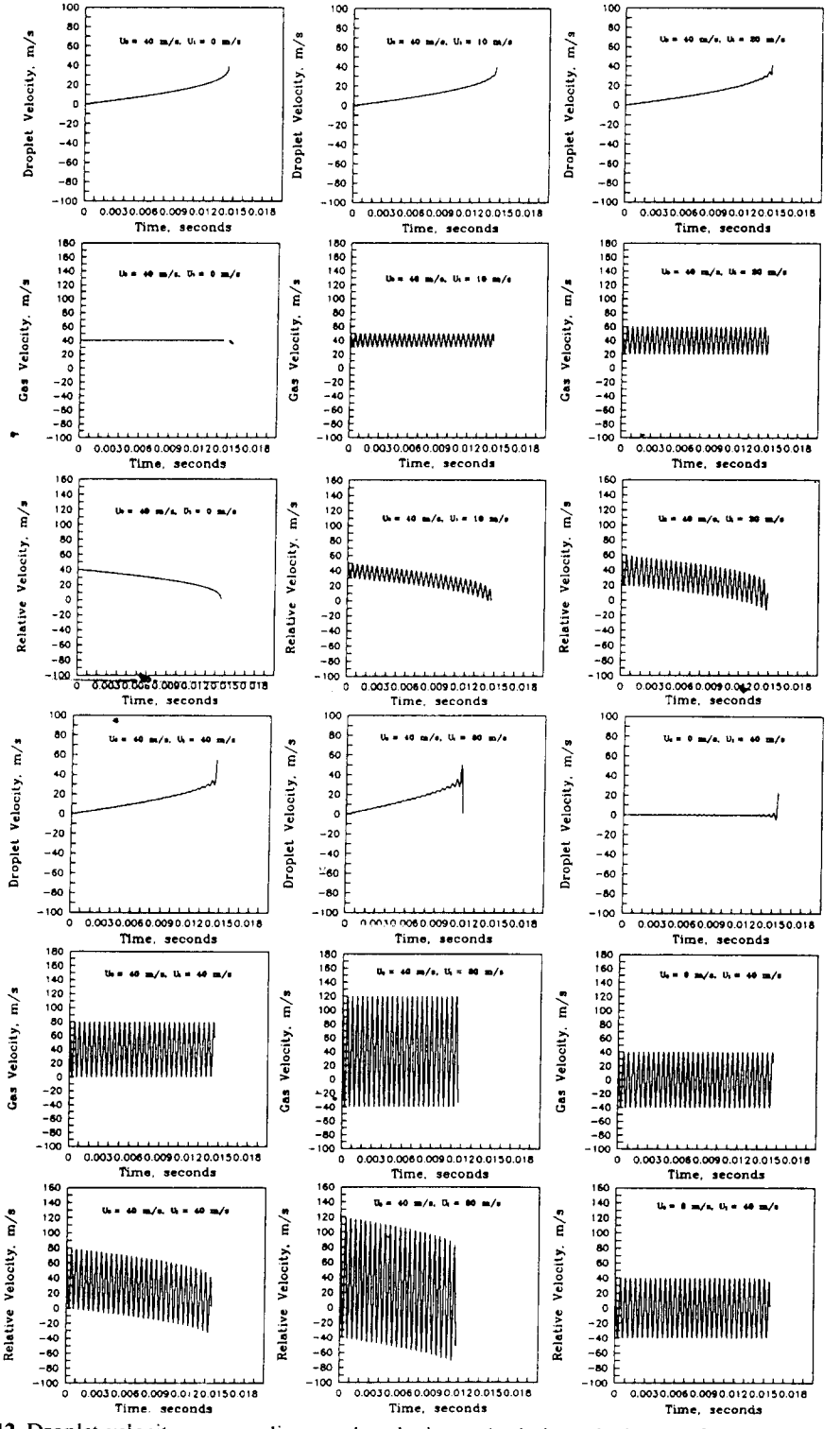

Fig. 12 Droplet velocity, surrounding steady velocity and relative velocity as a function of time for various values of U_0 and U_1 : f=2000 Hz, $d_0 = 105\ \mu m$

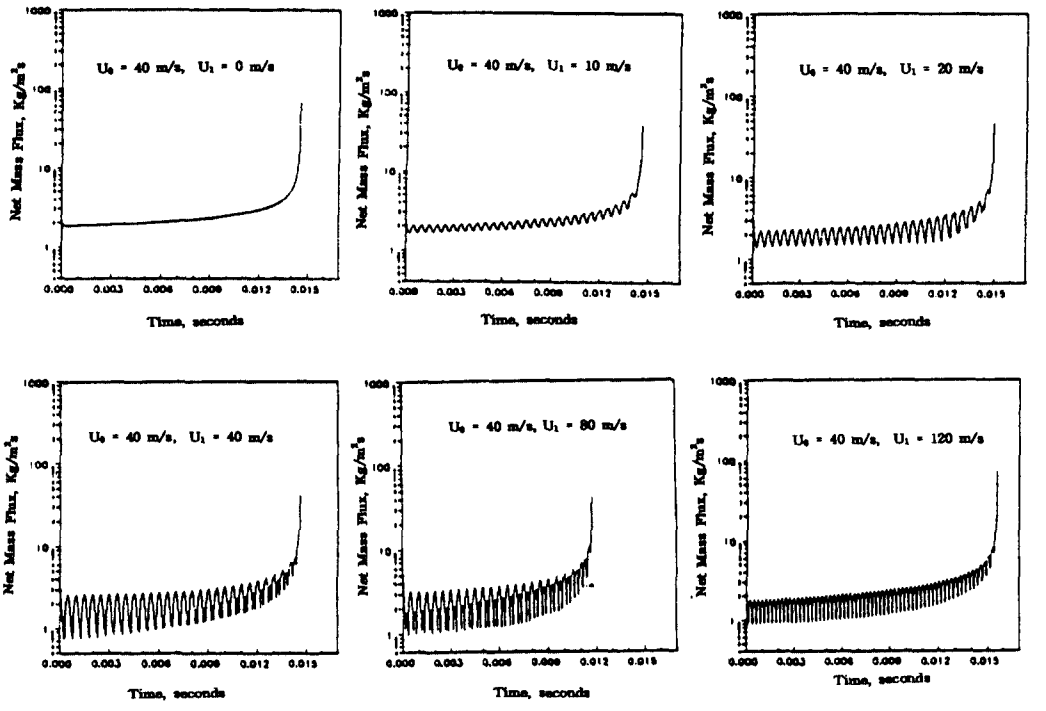

Fig. 13 Net mass flux as a function of time for various values of U_0 and U_1 : f=2000 Hz, d_0=105 μm

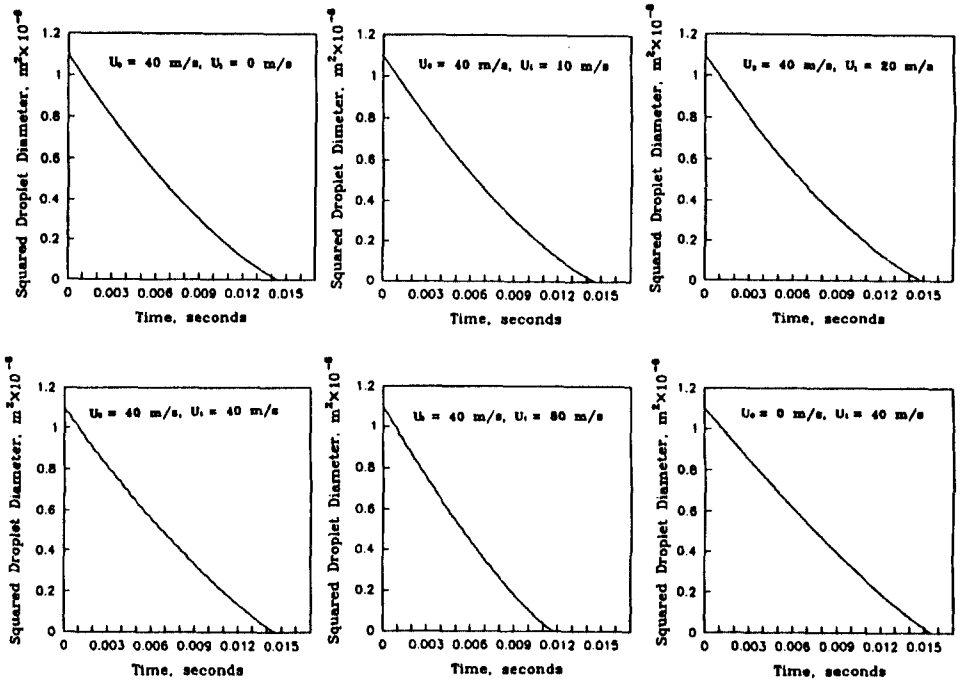

Fig. 14 Squared droplet diameter as a function of time for various values of U_0 and U_1 : f=2000 Hz, d_0=105 μm

shown in Figs. 13 and 14. Droplet entrainment decreases with increasing frequencies, resulting in slightly decreasing combustion time. The combustion times for $U_0=40$ and $f=2000$ Hz are 14.5 ms($U_1=0$), 14.64 ms($U_1=10$), 14.92 ms($U_1=20$), 14.60 ms($U_1=40$) and 11.73 ms($U_1=80$), respectively.

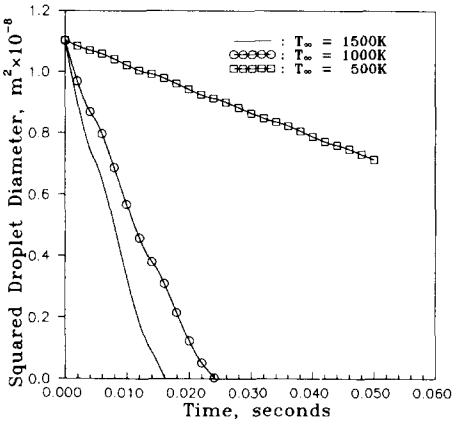

Fig. 15 Squared droplet diameter as a function of time for ambient temperatures of 500, 1000 and 15000K : $U_0=0$, $U_1=40$ m/s, f=50 Hz, $d_0=105$ μm

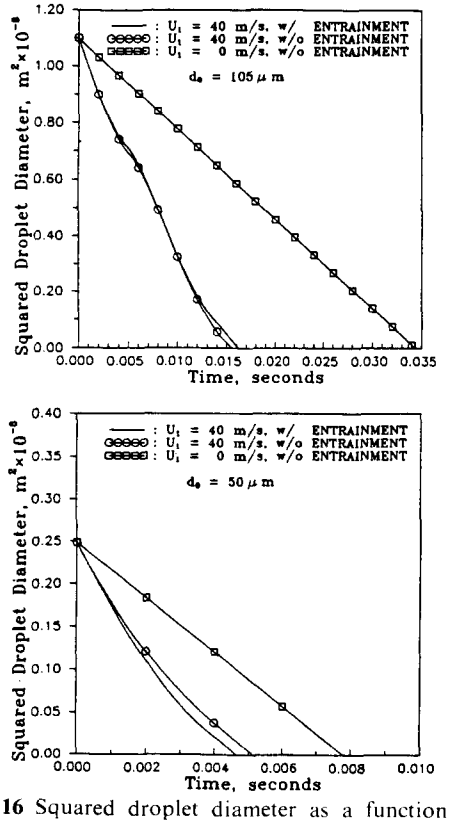

Fig. 16 Squared droplet diameter as a function of time for initial diameters of 50 and 105 μm : $U_0=0$, $U_1=40$ m/s, f=50 Hz

The effects of ambient temperature(T_∞) on droplet combustion are shown in Fig. 15. The heat and mass transfer from and to the burning droplet decrease with decreasing ambient temperature, resulting in the increase in the combustion time. The initial droplet diameter varies from 105 to 50 μm in order to consider the effects of droplet diameter on droplet combustion. The overall combustion phenomena for $d_0=50$ μm are similar to those for $d_0=105$ μm, comparing the results with droplet entrainment to those without entrainment and to those in the quiescent ambient conditions, as shown in Fig. 16. The droplet combustion time decreases with decreasing droplet diameter.

4. Summary and Conclusions

The combustion of a single droplet entrained in the oscillating flow with and without a steady velocity is investigated. The effects of droplet entrainment, frequency, the amplitude of oscillating velocity, velocity ratio U_1/U_0, ambient temperature and droplet size on the combustion of a single droplet were investigated.

(1) In the presence of the oscillating flow, the entrainment of burning droplet increases and the phase lag between the droplet movement and the oscillating flow decreases with decreasing droplet diameter and with decreasing frequency. At 50 Hz, the droplet is entrained in the oscillating flow with a phase lag. Due to this phase lag, the relative velocity between the flow and the droplet has an amplitude slightly lower than that of oscillating flow U during a significantly long time. The combustion time with entrainment is 3.7% longer than the case of no entrainment. If the frequency is increased to 2000 Hz, the droplet entrainment is very small. Therefore, the relative velocity is almost the same as the oscillating velocity, giving almost the same combustion time with and without droplet entrainment. The burning history of droplet entrained in an oscillating

flow is not governed by the d^2-law, unlike to the case under quiescent ambient conditions.

(2) When the steady velocity U_0 is higher than the oscillating component U_1, the combustion time increases slightly with increasing U_1 due to the decrease in heat and mass transfer from and to the burning droplet, as compared to the case of steady flow only. When U_1 is larger than U_0, the combustion time decreases with increasing U_1 over U_0, showing the enhancement of droplet combustion in the presence of oscillating flow induced by the high intensity acoustic fields.

(3) In the presence of oscillating flow, the combustion time decreases with increasing amplitude of oscillating flow, increasing ambient temperature and decreasing initial droplet diameter.

References

Aggarwal, S. K. and Sirignano, W. A., 1985, "Unsteady Spray Flame Propagation in a Closed Volume," *Combustion and Flame*, Vol. 62, pp. 69~84.

Baxi, C. B. and Ramachandran, A., 1969, "Effect of Vibration on Heat Transfer from Spheres," *ASME J. of Heat Transfer*, pp. 337~344.

Chao, B. H., Matalon, M. and Law, C. K., 1985, "Gas-Phase Transient Diffusion in Droplet Ignition," *Combustion and Flame*, Vol. 59, pp. 43~51.

Chung, S. H. and Law, C. K., 1983, "Structure and Extinction of Convective Diffusion Flames with General Lewis Numbers," *Combustion and Flame*, Vol. 52, pp. 59~70.

Faeser, R. J., 1984, "Acoustic Enhancement of Pulverized Coal Combustion," *ASME Paper*, 84-WA/NCA-18.

Faeth, G. M., 1983, "Evaporation and Combustion of Sprays," *Prog. Energy Combust. Sci.*, Vol. 9, pp. 1~76.

Fernandez-Pello, A. C. and Law, C. K., 1982, "A Theory for the Free-Convective Burning of a Condensed Fuel Particle," *Combustion and Flame*, Vol. 44, pp. 97~112.

Gibert, H. and Angelino, 1974, "Transferts De Matiere Entre Une Sphere Soumise A Des Vibrations Et Un Liquide En Mouvement," *Int'l J. of Heat and Mass Transfer*, Vol. 17, pp. 625~632.

Ha, M. Y., 1990, A Theoretical Study of Augmentation of Particle Combustion via Acoustic Enhancement of Heat and Mass Transfer, Ph. D. Thesis, The Pennsylvania State University State College, Pennsylvania.

Ha, M. Y. and Yavuzkurt S., 1991, "Combustion of a Single Carbon or Char Particle in the Presence of High Intensity Acoustic Fields," *Combustion and Flame*, Vol. 86, pp. 33~46.

Ha, M. Y. and Yavuzkurt, S., 1993, "A theoretical Investigation of Acoustic Enhancement of Heat and Mass Transfer-Ⅱ. Oscillating Flow With a Steady Velocity Component," *Intl J. of Heat and Mass Transfer*, Vol. 36, No. 8, pp. 2193~2202.

Kanury, A. M., 1977, *Introduction to Combustion Phenomena*, 2nd Edition, Gordon and Breach Publisher.

Koopmann, G. K., Scaroni, A. W., Yavuzkurt, S., Ramanchandran, P. and Ha, M. Y., 1989, "Acoustically Enhanced Combustion of Micronized Coal Water Slurry Fuel," *Final Report for Department of Energy*, DE-RA-86MC23257.

Larsen, P. S. and Jensen, J. W., 1978, "Evaporation Rates of Drops in Forced Convection with Superposed Transverse Sound Field," *Intl. J. Heat and Mass Transfer*, Vol. 21, pp. 511~517.

Law, C. K., 1982, "Recent Advances in Droplet Vaporization and Combustion," *Prog. Energy Combust. Sci.*, Vol. 8, pp. 171~201.

Marthelli, R. C. and Boelter, L. M. K., 1939, "The Effect of Vibration on Heat Transfer by Free Convection from a Horizontal Cylinder," *Proc. 5th International Congress of Applied Mechanics*, pp. 578~584.

Mori, Y., Imabayashi, M., Hijikata, K. and Yoshida, Y., 1969, "Unsteady Heat and Mass Transfer from Spheres," *Intl. J. Heat Mass Transfer*, Vol. 12, pp. 571~585.

Patankar, S. V., 1980, *Numerical Heat Transfer and Fluid Flow*, 1st Edition, Hemisphere, Washington D.C.

Rawson, S. A., 1988, "An Experimental Investigation of the Influence of High Intensity Acoustics on Heat and Mass Transfer Rates from

Spheres as Related to Coal-Water Slurry Fuel Combustion Enhancement," M. S. Thesis, The Pennsylvania State University State College, Pennsylvania.

Smith, P. J., Fletcher, T. H. and Smoot, L. D., 1985, "Prediction and Measurement of Entrained Flow Coal Gasification Process, Volume Ⅱ, User's Manual for a Computer Program for Two-Dimensional Coal Gasification or Combustion(PCGC2)," *Final Report to DOE/METC under Contract No. DE-AC21-81MC16518.*

Van Doormaal, J. P. and Raithby, G. D., 1984, "Enhancement of the Simple Method for Predicting Incompressible Fluid Flow," *Numerical Heat Transfer,* Vol. 7, pp. 147~163.

Wiliams, A., 1976, "Fundamentals of Oil Combustion," *Prog. Energy Combust Sci.,* Vol. 2, pp. 167~179.

Wu, X., Law, C. K. and Fernandez-Pello, A. C., 1982, "A Unified Criterion for the Convective Extinction of Fuel Particles," *Combustion and Flame,* Vol. 44, pp. 113~124.

Yavuzkurt, S. and Ha, M. Y., 1991, "A Model of the Enhancement of Combustion of Coal Water Slurry Fuels Using High Intensity Acoustic Fields," *ASME J. of Energy Resources Technology,* Vol. 113, pp. 268~276.

Yavuzkurt, S., Ha, M. Y., Koopmann, G. and Scaroni, A. W., 1991, "A Model of the Enhancement of Coal Combustion Using High Intensity Acoustic Fields," *ASME J. of Energy Resources & Technology,* Vol. 113, pp. 277~285.

Zinn, B. T., 1984, "State of the Art and Research Needs of Pulsating Combustion," *ASME Paper, 84-WA/NCA-19.*